2022 EAGE ANNUAL
83RD CONFERENCE & EXHIBITION
MADRID I SPAIN

ELASTODYNAMIC MARCHENKO GREEN'S FUNCTION RETRIEVAL FROM TWO-SIDED REFLECTION AND TRANSMISSION DATA

J. Van der Neut[1], J. Brackenhoff[2], G. Meles[3], E. Slob[1], K. Wapenaar[1]

[1] Delft University of Technology; [2] ETH Zurich; [3] University of Lausanne

Summary

Green's functions in an unknown elastic layered medium can be retrieved from single-sided reflection data by solving a Marchenko equation. This methodology requires a priori knowledge of all forward-scattered (non-converted and converted) waveforms. Moreover, the medium should satisfy stringent monotonicity conditions, which are often not met in realistic scenarios. In this contribution, we show that the situation is significantly less cumbersome if two-sided reflection and transmission data are recorded (for instance in laboratory settings). A novel methodology is presented to retrieve elastodynamic Green's functions from such data. Apart from the two-sided reflection and transmission responses, our methodology requires knowledge of the direct non-converted PP- and SS-transmissions (a priori knowledge of forward-scattered converted waveforms is not needed). We demonstrate the success of our methodology by conducting a numerical experiment in an elastic layered medium that violates the monotonicity conditions of the Marchenko equation for single-sided reflection data. The limitations of the methodology and the sensitivity to errors in our initial estimates require further investigation.

Elastodynamic Marchenko Green's function retrieval from two-sided reflection and transmission data

Introduction

It is well-known that Green's functions between an acquisition surface S and a specific location $\boldsymbol{x}$ in an unknown acoustic layered medium can be retrieved by solving a Marchenko equation (Slob et al., 2014). The Marchenko methodology requires a broadband single-sided reflection response and knowledge of the direct wavefield as it would propagate between S and $\boldsymbol{x}$. Equivalent representations have been derived for elastodynamic wave propagation (Wapenaar and Slob, 2014; da Costa Filho et al., 2014). However, the utilization of these representations for Green's function retrieval requires knowledge of all forward-scattered arrivals between S and $\boldsymbol{x}$, which is infeasible in practice. Moreover, successful implementation requires the elastic medium to satisfy stringent monotonicity conditions, which are often violated in realistic scenarios (Reinicke et al., 2020). In this contribution, we show that the requirements for elastodynamic Green's function retrieval with the Marchenko equation can be weakened significantly when two-sided reflection and transmission data are recorded.

Modified system of Marchenko equations

We consider a layered elastic medium that is bound from above by an upper acquisition surface S_U and from below by a lower acquisition surface S_L. The medium properties are constant above S_U and below S_L. Our goal is to retrieve the upgoing Green's functions $\boldsymbol{G}_U^{-+}$ and $\boldsymbol{G}_U^{--}$ at S_U, due to a source at a specific depth z in the medium. Here, $\boldsymbol{G}_U^{-+}$ contains all downward-radiating components, while $\boldsymbol{G}_U^{--}$ contains all upward-radiating components. In our notation, each bold quantity represents a *2x2* matrix, containing the $\begin{pmatrix} PP & PS \\ SP & SS \end{pmatrix}$-components in the (τ, p)-domain (where τ is the intercept time and p is the ray parameter). Let $\boldsymbol{\mathcal{R}}_U = \begin{pmatrix} \mathcal{R}_U^{PP} & \mathcal{R}_U^{PS} \\ \mathcal{R}_U^{SP} & \mathcal{R}_U^{SS} \end{pmatrix}$ be an operator that convolves an arbirary wavefield with the reflection response at S_U, while $\boldsymbol{\mathcal{Z}}$ is an operator for reversing the time and rayparameter. Moreover, we introduce the down- and upgoing focusing functions $\boldsymbol{F}_U^{+}$ and $\boldsymbol{F}_U^{-}$, respectively, which obey a specific focusing condition at depth z; see Wapenaar and Slob (2014) for details. Let $\boldsymbol{G}_{Ud}^{--} = \begin{pmatrix} G_{Ud}^{PP} & 0 \\ 0 & 0 \end{pmatrix}$ be the first event of $\boldsymbol{G}_U^{--}$, being the direct non-converted *PP*-transmission, while $\boldsymbol{G}_{Um}^{--} = \boldsymbol{G}_U^{--} - \boldsymbol{G}_{Ud}^{--}$ is referred to as the Green's function coda (note that our definition of $\boldsymbol{G}_{Um}^{--}$ includes all other direct and forward-scattered waves, i.e. the non-converted *SS*-transmission G_{Ud}^{SS} and all converted waveforms). Let $\boldsymbol{F}_{Ud}^{+} = \begin{pmatrix} 0 & 0 \\ 0 & F_{Ud}^{SS} \end{pmatrix}$ be the first event of $\boldsymbol{F}_U^{+}$, being the direct non-converted *SS*-transmission, while $\boldsymbol{F}_{Um}^{+} = \boldsymbol{F}_U^{+} - \boldsymbol{F}_{Ud}^{+}$ is referred to as the focusing function coda (note that our definition of $\boldsymbol{F}_{Um}^{+}$ includes all other direct and forward-scattered waves, i.e. the non-converted *PP*-transmission F_{Ud}^{PP} and all converted waveforms). These definitions allow us to cast the convolution- and correlation-based representations of Wapenaar and Slob (2014) as the upper two rows of the following system of equations:

$$\begin{pmatrix} \boldsymbol{\mathcal{R}}_U \boldsymbol{F}_{Ud}^{+} \\ -\boldsymbol{G}_{Ud}^{--} - \boldsymbol{\mathcal{Z}} \boldsymbol{F}_{Ud}^{+} \\ \boldsymbol{\mathcal{R}}_L \boldsymbol{F}_{Ld}^{-} \\ -\boldsymbol{G}_{Ld}^{++} - \boldsymbol{\mathcal{Z}} \boldsymbol{F}_{Ld}^{-} \end{pmatrix} - \begin{pmatrix} \boldsymbol{G}_U^{-+} \\ \boldsymbol{G}_{Um}^{--} \\ \boldsymbol{G}_L^{+-} \\ \boldsymbol{G}_{Lm}^{++} \end{pmatrix} = \begin{pmatrix} \boldsymbol{I} & -\boldsymbol{\mathcal{R}}_U & \boldsymbol{0} & \boldsymbol{0} \\ -\boldsymbol{\mathcal{R}}_U \boldsymbol{\mathcal{Z}} & \boldsymbol{\mathcal{Z}} & \boldsymbol{0} & \boldsymbol{0} \\ \boldsymbol{0} & \boldsymbol{0} & \boldsymbol{I} & -\boldsymbol{\mathcal{R}}_L \\ \boldsymbol{0} & \boldsymbol{0} & -\boldsymbol{\mathcal{R}}_L \boldsymbol{\mathcal{Z}} & \boldsymbol{\mathcal{Z}} \end{pmatrix} \begin{pmatrix} \boldsymbol{F}_U^{-} \\ \boldsymbol{F}_{Um}^{+} \\ \boldsymbol{F}_L^{+} \\ \boldsymbol{F}_{Lm}^{-} \end{pmatrix}. \tag{1}$$

In this system, the lower two rows are similar equations for wavefields at the lower boundary S_L. Let $\boldsymbol{\Theta}_U$ be a time-symmetric window function that preserves all data in the interval $\left[-t_{Ud}^{PP} - t_\varepsilon, t_{Ud}^{PP} + t_\varepsilon\right]$, while it mutes all data outside this interval. Here, t_{Ud}^{PP} is the traveltime of the direct non-converted *PP*-transmission and t_ε is a small time shift that accounts for the finite frequency content of the data (Slob et al., 2014). A similar window $\boldsymbol{\Theta}_L$ is constructed for the wavefields at the lower boundary. We emphasize that these time windows are based on the non-converted *PP*-traveltime only, unlike in previous publications, where the windows are typically based on the first onsets of the *PP*-, *SP*-, *PS*- and *SS*-transmissions. Applying $\mathrm{diag}(\boldsymbol{\Theta}_U, \boldsymbol{\Theta}_U, \boldsymbol{\Theta}_L, \boldsymbol{\Theta}_L)$ to both sides of equation (1) yields

$$\begin{pmatrix} \boldsymbol{\Theta}_U \boldsymbol{\mathcal{R}}_U \boldsymbol{F}_{Ud}^{+} \\ -\boldsymbol{G}_{Ud}^{--} \\ \boldsymbol{\Theta}_L \boldsymbol{\mathcal{R}}_L \boldsymbol{F}_{Ld}^{-} \\ -\boldsymbol{G}_{Ld}^{++} \end{pmatrix} = \begin{pmatrix} \boldsymbol{\Theta}_U & -\boldsymbol{\Theta}_U \boldsymbol{\mathcal{R}}_U & \boldsymbol{0} & \boldsymbol{0} \\ -\boldsymbol{\Theta}_U \boldsymbol{\mathcal{R}}_U \boldsymbol{\mathcal{Z}} & \boldsymbol{\Theta}_U \boldsymbol{\mathcal{Z}} & \boldsymbol{0} & \boldsymbol{0} \\ \boldsymbol{0} & \boldsymbol{0} & \boldsymbol{\Theta}_L & \boldsymbol{\Theta}_L \boldsymbol{\mathcal{R}}_L \\ \boldsymbol{0} & \boldsymbol{0} & -\boldsymbol{\Theta}_L \boldsymbol{\mathcal{R}}_L \boldsymbol{\mathcal{Z}} & \boldsymbol{\Theta}_L \boldsymbol{\mathcal{Z}} \end{pmatrix} \begin{pmatrix} \boldsymbol{F}_U^{-} \\ \boldsymbol{F}_{Um}^{+} \\ \boldsymbol{F}_L^{+} \\ \boldsymbol{F}_{Lm}^{-} \end{pmatrix}. \tag{2}$$

Let's assume that the four spikes F_{Ud}^{SS}, G_{Ud}^{PP}, F_{Ld}^{SS} and G_{Ld}^{PP} that are required to construct the left-hand side of this equation are known *a priori*. Now, we may try to resolve the unknown quantity $(\boldsymbol{F}_U^{-}, \boldsymbol{F}_{Um}^{+}, \boldsymbol{F}_L^{+}, \boldsymbol{F}_{Lm}^{-})^T$ in the right-hand-side by inversion. Unfortunately, all components of the unkown that reside outside the intervals $\left[-t_{Ud}^{PP} - t_\varepsilon, t_{Ud}^{PP} + t_\varepsilon\right]$ and $\left[-t_{Ld}^{PP} - t_\varepsilon, t_{Ld}^{PP} + t_\varepsilon\right]$ (i.e. the forward-scattered waveforms and events that violate the monotonicity conditions of Reinicke et al. (2020)) can generally not be recovered by this procedure. To overcome this limitation, we couple the wavefields at the upper and lower boundary (which are not coupled in equation (2)) by incorporating auxiliary transmission data in the next section.

System of auxiliary equations

Let $\boldsymbol{\mathcal{T}}_{UL}$ and $\boldsymbol{\mathcal{T}}_{LU}$ be transmission operators (from S_L to S_U and from S_U to S_L, respectively), both having a similar structure as $\boldsymbol{\mathcal{R}}_U$ and $\boldsymbol{\mathcal{R}}_L$. Now, four more representations can be derived, which we can cast into the following system:

$$\begin{pmatrix} \boldsymbol{0} \\ \boldsymbol{G}_{Ud}^{--} + \boldsymbol{\mathcal{T}}_{UL} \boldsymbol{F}_{Ld}^{-} \\ \boldsymbol{0} \\ \boldsymbol{G}_{Ld}^{++} + \boldsymbol{\mathcal{T}}_{LU} \boldsymbol{F}_{Ud}^{+} \end{pmatrix} + \begin{pmatrix} \boldsymbol{G}_U^{-+} \\ \boldsymbol{G}_{Um}^{--} \\ \boldsymbol{G}_L^{+-} \\ \boldsymbol{G}_{Lm}^{++} \end{pmatrix} = \begin{pmatrix} \boldsymbol{0} & \boldsymbol{0} & -\boldsymbol{\mathcal{T}}_{UL} \boldsymbol{\mathcal{Z}} & \boldsymbol{0} \\ \boldsymbol{0} & \boldsymbol{0} & \boldsymbol{0} & -\boldsymbol{\mathcal{T}}_{UL} \\ -\boldsymbol{\mathcal{T}}_{LU} \boldsymbol{\mathcal{Z}} & \boldsymbol{0} & \boldsymbol{0} & \boldsymbol{0} \\ \boldsymbol{0} & -\boldsymbol{\mathcal{T}}_{LU} & \boldsymbol{0} & \boldsymbol{0} \end{pmatrix} \begin{pmatrix} \boldsymbol{F}_U^{-} \\ \boldsymbol{F}_{Um}^{+} \\ \boldsymbol{F}_L^{+} \\ \boldsymbol{F}_{Lm}^{-} \end{pmatrix}. \tag{3}$$

When we apply $\mathrm{diag}(\boldsymbol{\Theta}_U, \boldsymbol{\Theta}_U, \boldsymbol{\Theta}_L, \boldsymbol{\Theta}_L)$ to this result, we obtain a system of auxiliary equations:

$$\begin{pmatrix} \boldsymbol{0} \\ \boldsymbol{G}_{Ud}^{--} + \boldsymbol{\Theta}_U \boldsymbol{\mathcal{T}}_{UL} \boldsymbol{F}_{Ld}^{-} \\ \boldsymbol{0} \\ \boldsymbol{G}_{Ld}^{++} + \boldsymbol{\Theta}_L \boldsymbol{\mathcal{T}}_{LU} \boldsymbol{F}_{Ud}^{+} \end{pmatrix} = \begin{pmatrix} \boldsymbol{0} & \boldsymbol{0} & -\boldsymbol{\Theta}_U \boldsymbol{\mathcal{T}}_{UL} \boldsymbol{\mathcal{Z}} & \boldsymbol{0} \\ \boldsymbol{0} & \boldsymbol{0} & \boldsymbol{0} & -\boldsymbol{\Theta}_U \boldsymbol{\mathcal{T}}_{UL} \\ -\boldsymbol{\Theta}_L \boldsymbol{\mathcal{T}}_{LU} \boldsymbol{\mathcal{Z}} & \boldsymbol{0} & \boldsymbol{0} & \boldsymbol{0} \\ \boldsymbol{0} & -\boldsymbol{\Theta}_L \boldsymbol{\mathcal{T}}_{LU} & \boldsymbol{0} & \boldsymbol{0} \end{pmatrix} \begin{pmatrix} \boldsymbol{F}_U^{-} \\ \boldsymbol{F}_{Um}^{+} \\ \boldsymbol{F}_L^{+} \\ \boldsymbol{F}_{Lm}^{-} \end{pmatrix}. \tag{4}$$

We may try to invert equations (2) and (4) jointly for the unknown $(\boldsymbol{F}_U^{-}, \boldsymbol{F}_{Um}^{+}, \boldsymbol{F}_L^{+}, \boldsymbol{F}_{Lm}^{-})^T$. However, this procedure still suffers from the actions of window operators $\boldsymbol{\Theta}_U$ and $\boldsymbol{\Theta}_L$, which effectively reduce the rank of the system's overall matrix. We aim to overcome this limitation by deriving yet another system of equations in the following section.

System of coupled equations

Note that the Green's functions in the left-hand sides of equations (1) and (3) can be eliminated by adding these equations together. This leads to the following system of coupled equations:

$$\begin{pmatrix} \boldsymbol{\mathcal{R}}_U \boldsymbol{F}_{Ud}^{+} \\ \boldsymbol{\mathcal{T}}_{UL} \boldsymbol{F}_{Ld}^{-} - \boldsymbol{\mathcal{Z}} \boldsymbol{F}_{Ud}^{+} \\ \boldsymbol{\mathcal{R}}_L \boldsymbol{F}_{Ld}^{-} \\ \boldsymbol{\mathcal{T}}_{LU} \boldsymbol{F}_{Ud}^{+} - \boldsymbol{\mathcal{Z}} \boldsymbol{F}_{Ld}^{-} \end{pmatrix} = \begin{pmatrix} \boldsymbol{I} & -\boldsymbol{\mathcal{R}}_U & -\boldsymbol{\mathcal{T}}_{UL} \boldsymbol{\mathcal{Z}} & \boldsymbol{0} \\ -\boldsymbol{\mathcal{R}}_U \boldsymbol{\mathcal{Z}} & \boldsymbol{\mathcal{Z}} & \boldsymbol{0} & -\boldsymbol{\mathcal{T}}_{UL} \\ -\boldsymbol{\mathcal{T}}_{LU} \boldsymbol{\mathcal{Z}} & \boldsymbol{0} & \boldsymbol{I} & -\boldsymbol{\mathcal{R}}_L \\ \boldsymbol{0} & -\boldsymbol{\mathcal{T}}_{LU} & -\boldsymbol{\mathcal{R}}_L \boldsymbol{\mathcal{Z}} & \boldsymbol{\mathcal{Z}} \end{pmatrix} \begin{pmatrix} \boldsymbol{F}_U^{-} \\ \boldsymbol{F}_{Um}^{+} \\ \boldsymbol{F}_L^{+} \\ \boldsymbol{F}_{Lm}^{-} \end{pmatrix} \tag{5}$$

One approach would be to invert equation (5) directly, without intervention of the window operators. However, this procedure does not use the information in equations (1) and (3) in an optimal sense, as we may have accidently reduced the system's row space by adding the equations together. Instead, we propose to invert equations (2), (4) and (5) together for $(\boldsymbol{F}_U^{-}, \boldsymbol{F}_{Um}^{+}, \boldsymbol{F}_L^{+}, \boldsymbol{F}_{Lm}^{-})^T$, which we enforce to be zero outside the intervals $\left(-t_{Ud}^{SS} + t_\varepsilon, t_{Ud}^{SS} - t_\varepsilon\right)$ and $\left(-t_{Ld}^{SS} + t_\varepsilon, t_{Ld}^{SS} - t_\varepsilon\right)$ during inversion. Here, t_{Ud}^{SS} and t_{Ld}^{SS} are the traveltimes of the direct non-converted *SS*-transmissions from the focal depth z to the upper and lower boundary, respectively.

Numerical example

To illustrate the effectiveness of the proposed methodology, we conduct a numerical experiment. Synthetic data are computed in an elastic medium, which is shown in Figure 1(a). In this medium, both monotonicity conditions of Reinicke et al. (2020) are violated. Our goal is to retrieve Green's functions as if there were a source at the focal depth $z = 1m$ with rayparameter $p = 0.2ms/m$. As input data, we compute two-sided reflection and transmission data with this rayparameter, using a zero-phase wavelet with a central frequency of $50kHz$ (based on this wavelet, we set $t_\varepsilon = 18\mu s$). Apart from these data, our scheme requires four band-limited pulses G_{Ud}^{PP}, F_{Ud}^{SS}, G_{Ld}^{PP} and F_{Ld}^{SS}, which are also precomputed. Two of these pulses are shown in figures 1(b) and 1(c). The cyan lines in these (and subsequent) figures denote the traveltimes $-t_{Ud}^{PP} - t_\varepsilon$ and $t_{Ud}^{PP} + t_\varepsilon$, which are used to construct the window operator $\boldsymbol{\Theta}_U$. The magenta lines denote $-t_{Ud}^{SS} + t_\varepsilon$ and $t_{Ud}^{SS} - t_\varepsilon$, marking the interval $\left(-t_{Ud}^{SS} + t_\varepsilon, t_{Ud}^{SS} - t_\varepsilon\right)$ where the unknown components of the focusing functions are allowed to be non-zero. The latter is enforced during the inversion by incorporating a restriction operator $\boldsymbol{\Xi}$ in our formulation, muting all data outside the prescribed interval. Another operator $\boldsymbol{Q}$ is introduced for convolution with the source wavelet. We use these operators to rewrite $(\boldsymbol{F}_U^-, \boldsymbol{F}_{Um}^+, \boldsymbol{F}_L^+, \boldsymbol{F}_{Lm}^-)^T$ as $\boldsymbol{Q\Xi}\left(\widehat{\boldsymbol{F}}_U^-, \widehat{\boldsymbol{F}}_{Um}^+, \widehat{\boldsymbol{F}}_L^+, \widehat{\boldsymbol{F}}_{Lm}^-\right)^T$, where the hat denotes a wavelet-free representation, which is assumed to be relatively sparse in the time domain. We exploit this sparsity (Haindl et al., 2021) by solving the three systems of equations (2), (4) and (5) jointly for $\left(\widehat{\boldsymbol{F}}_U^-, \widehat{\boldsymbol{F}}_{Um}^+, \widehat{\boldsymbol{F}}_L^+, \widehat{\boldsymbol{F}}_{Lm}^-\right)^T$, using the solver *SPGL1* (van den Berg and Friedlander, 2008). We run 100 iterations with this solver, where we set the initial sparsity parameter equal to the $L1$-norm of a solution in an equivalent homogeneous medium (since we know that the solution in a heterogeneous medium should exceed this level). After inversion, we convolve the recovered sparse waveforms with the source wavelet. In figures 2 and 3, we compare $\boldsymbol{F}_U^+ = \boldsymbol{F}_{Ud}^+ + \boldsymbol{F}_{Um}^+$ and $\boldsymbol{F}_U^-$ as retrieved by this procedure (in dashed red) with equivalent focusing functions that have been computed by direct modeling (in black). We observe that all forward-scattered and reflected waveforms have been recovered, although some weaker arrivals have been underestimated. In figures 4 and 5, we show the Green's functions $\boldsymbol{G}_U^{--} = \boldsymbol{G}_{Ud}^{--} + \boldsymbol{G}_{Um}^{--}$ and $\boldsymbol{G}_U^{-+}$, which we have constructed from the retrieved focusing functions by rearranging equation (3). Most waveforms have been recovered, where we note that some amplitudes have been underestimated. Note that there is a significant overlap of the Green's functions and time-reversed focusing functions on the interval $\left(t_{Ud}^{PP}, t_{Ud}^{SS}\right)$. This overlap hampers applications with the single-sided Marchenko equation (Reinicke et al., 2020), which we overcame by incorporating transmission data.

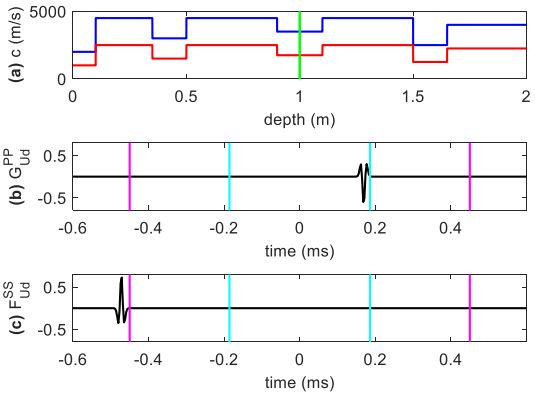

Figure 1 ***(a)*** *c_P (in blue) and c_S (in red). Density is constant $\rho = 2000kg\,m^{-3}$. The green line denotes the focal depth $z = 1m$.* ***(b)*** *Direct non-converted PP-transmission at the upper boundary G_{Ud}^{PP}, which is used as input.* ***(c)*** *Inverse direct non-converted SS-transmission at the upper boundary F_{Ud}^{SS}, which is used as input. The cyan lines mark the traveltimes $\pm t_{Ud}^{PP} \pm t_\varepsilon$, while the magenta lines mark $\pm t_{Ud}^{SS} \mp t_\varepsilon$.*

Discussion

We have presented a methodology to retrieve Green's functions in a layered elastic medium from two-sided reflection and transmission data. Our method does not depend on *a priori* knowledge of forward-scattered converted waveforms. We have demonstrated the method successfully on a particular model that violates the monotonicity conditions of Reincike et al. (2020). Its performance and limitations on arbitrary elastic models remains to be investigated, as is the sensitivity of our method for the phases and amplitudes of the initial spikes F_{Ud}^{SS}, G_{Ud}^{PP}, F_{Ld}^{SS} and G_{Ld}^{PP}. In its current form, the method requires sufficient bandwidth with respect to the layer thicknesses in the medium. This limitation might be overcome by incorporating insights of the augmented focusing function of Dukalski et al. (2019). Moreover, the methodology could be extended to viscoelastic media, using insights from Slob (2016).

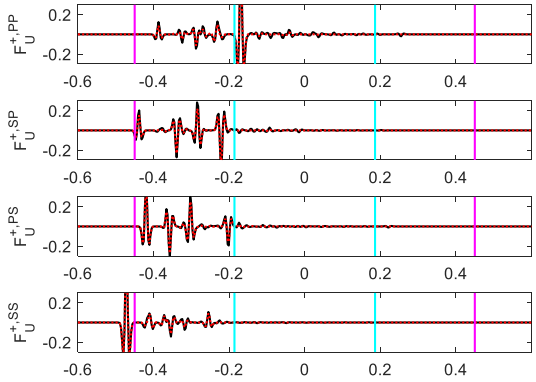

Figure 2 *Retrieved components of* $\boldsymbol{F}_U^+$ *(in dashed red), versus reference (in solid black).*

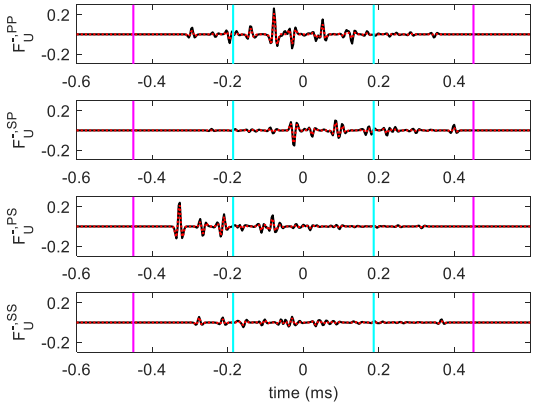

Figure 3 *Retrieved components of* $\boldsymbol{F}_U^-$ *(in dashed red), versus reference (in solid black).*

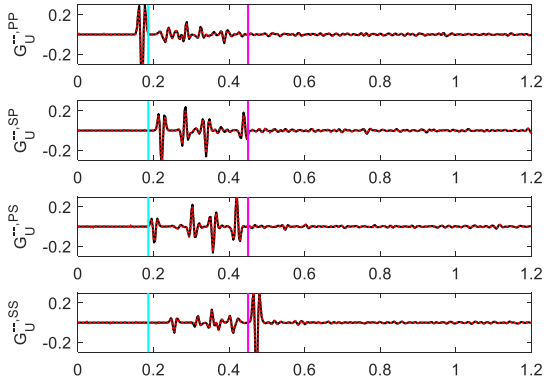

Figure 4 *Retrieved components of* $\boldsymbol{G}_U^{--}$ *(in dashed red), versus reference (in solid black).*

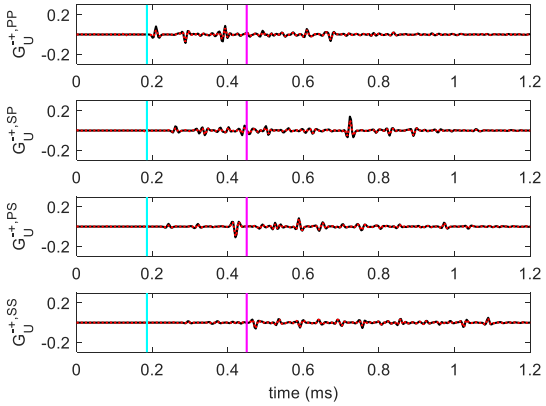

Figure 5 *Retrieved components of* $\boldsymbol{G}_U^{+-}$ *(in dashed red), versus reference (in solid black).*

Acknowledgements

The research of Kees Wapenaar, Joeri Brackenhoff and Giovani Meles has received funding from the European Research Council (grant no. 742703).

References

- da Costa Filho, C. A., Ravasi, M., Curtis, A., and Meles, G. A. [2014] Elastodynamic Green's function retrieval through single-sided Marchenko inverse scattering. *Physical Review E*, **90**, 063201.
- Dukalski, M., Mariani, E., and de Vos, K. [2019] Handling short-period scattering using augmented Marchenko autofocusing. *Geophyiscal Journal International*, **216**, 2129-2133.
- Haindl, C., Ravasi, M., and Broggini, F. [2021] Handling gaps in acquisition geometries - Improving Marchenko-based imaging using sparsity-promoting inversion and joint inversion of time-lapse data. *Geophysics*, **86**, S143-S154.
- Reinicke, C., Dukalski, M., and Wapenaar, K. [2020] Comparison of monotonicity challenges encountered by the inverse scattering series and the Marchenko demultiple method for elastic waves. *Geophysics*, **85**, Q11-Q26.
- Slob, E., Wapenaar, K., Broggini, F., and Snieder, R. [2014] Seismic reflector imaging using internal multiples with Marchenko-type equations. *Geophysics*, **79**, S63-S76.
- Slob, E. [2016] Green's function retrieval and Marchenko imaging in a dissipative acoustic medium. *Physical Review Letters*, **116**, 164301.
- van den Berg, E., and Friedlander, M. P. [2008] Probing the Pareto frontier for basis pursuit solutions. *SIAM Journal on Scientific Computing*, **31**, 890-912.
- Wapenaar, K., and Slob, E. [2014] On the Marchenko equation for multicomponent single-sided reflection data. *Geophysical Journal International*, **199**, 1367-1371.